Constitutive Overexpression of Pigment Epithelium–Derived Factor Inhibition of Ocular Melanoma Growth and Metastasis

Hua Yang[1] *and Hans E. Grossniklaus*[1,2,3]

Purpose. Pigment epithelium–derived factor (PEDF) is known to be an angiogenesis suppressor and to have antitumor effects. This study investigates whether constitutive overexpression of PEDF inhibits the growth and hepatic micrometastasis of ocular melanoma.

Methods. Real-time RT-PCR was used to detect endogenous PEDF expression in human uveal melanoma cell lines and mouse melanoma cells. A lentiviral vector containing a mouse PEDF expression sequence was constructed and transduced into mouse melanoma cells in vitro. Transgene expression was assessed by Western blot analysis. Angiogenesis and transendothelial migration assays were performed in constitutively stable PEDF-overexpressing cells and transduced lentiviral vector control cells. The size and microvessel density of the ocular tumor and the number of hepatic micrometastasis were compared between the mice inoculated with PEDF-overexpressing tumor cells and those mice with the control cell line.

Results. Four human uveal melanoma and three mouse melanoma cell lines were found to express PEDF mRNA. Endogenous overexpressing PEDF melanoma cells lost the ability to migrate and form tubes in vitro. In the animal experiment, the size of the ocular melanoma and the number of hepatic micrometastasis were decreased and microvessel density was also reduced in mice inoculated with constitutively overexpressing PEDF melanoma cells.

Conclusions. Lentivirus-mediated gene transfer of PEDF decreased the growth of ocular melanoma and its hepatic micrometastasis in a mouse ocular melanoma model. Dual antitumor/antiangiogenic activities of PEDF suggest that PEDF gene therapy may be considered an approach for the treatment of ocular melanoma. (*Invest Ophthalmol Vis Sci.* 2010;51:28–34) DOI:10.1167/iovs.09-4138

Uveal melanoma is the most common primary intraocular malignant tumor in adults and comprises nearly 85% of all ocular melanomas.[1] The worldwide incidence of uveal melanoma is 5.3 to 10.9 cases per million population, representing approximately 4.25% of all melanomas.[1] Despite progress in the diagnosis and treatment of the primary melanoma, the death rate from uveal melanoma has remained unchanged for the past 25 years.[1,2] Nearly 40% of primary uveal melanomas metastasize to the liver, ultimately leading to death.[1,2] Therefore, a better understanding of the cellular and molecular mechanisms of uveal melanoma progression is essential to develop novel and specific therapies to prevent or eliminate uveal melanoma metastasis.

Pigment epithelium–derived factor (PEDF) is a 50-kDa secreted glycoprotein that was first described in the late 1980s, after being identified and isolated from conditioned media of cultured primary human fetal retinal pigment epithelial cells.[3] PEDF is a noninhibitory member of the serpin (serine protease inhibitor) superfamily of proteins, and its gene, located on human chromosome 17p13.3, is highly conserved.[4,5] PEDF is endogenously produced, widely expressed in fetal and adult tissues, including the eye, liver, bone, adult brain, spinal cord, heart, and lung, and exhibits multiple and varied biological activities.[6–11] Expression of PEDF in the uvea and retina has been found in human and mouse eyes.[12–15] PEDF has been established as a potent antiangiogenic molecule and has been reported to inhibit choroidal neovascularization and to treat ocular diseases, such as age-related macular degeneration and proliferative diabetic retinopathy.[16–18] Uveal melanoma most often arises in the choroid and becomes vascularized, presumably via angiogenic mechanisms. In this study, we hypothesize that PEDF will inhibit uveal melanoma migration in vitro and angiogenesis in a mouse model of uveal melanoma, thus exhibiting direct and indirect antitumor activity.

Tumors may express low levels of PEDF.[19] Low levels or loss of expression of PEDF has been correlated with an increased incidence of metastasis and with poor prognoses in cutaneous melanoma, prostate carcinoma, pancreatic carcinoma, neuroblastoma, and glioma.[19–26] The antitumor effects of PEDF include antiangiogenesis, protumor differentiation, and direct tumor suppression by apoptosis.[25–29] Previous in vivo studies have shown that cutaneous melanoma expresses PEDF, and overexpression of PEDF in human cutaneous malignant melanoma cell lines has been achieved by stable transfection with PEDF plasmids and retroviral expression vectors, significantly reducing intratumoral microvessel density, primary tumor growth, and metastasis.[30,31] To date, the therapeutic potential of PEDF in uveal melanoma has not been tested. In this study, we demonstrate the expression of PEDF in mouse melanoma cell lines and human uveal melanoma cells and show that low expression of PEDF is associated with greater murine ocular melanoma and more hepatic micrometastases. We also demonstrate that constitutive overexpression of PEDF induced by a lentiviral vector-mediated PEDF gene inhibits tumor growth and hepatic micrometastasis.

From the Departments of [1]Ophthalmology and [2]Pathology and the [3]Winship Cancer Institute, Emory University School of Medicine, Atlanta, Georgia.

Supported by National Cancer Institute Grant R01CA126447 and National Eye Institute Grant R24EY017045. HEG is a recipient of the Research to Prevent Blindness Senior Scientific Investigator Award.

Submitted for publication June 12, 2009; revised July 14 and 27, 2009; accepted July 30, 2009.

Disclosure: **H. Yang**, None; **H.E. Grossniklaus**, None

Corresponding author: Hans E. Grossniklaus, L. F. Montgomery Ophthalmic Pathology Laboratory, BT428 Emory Eye Center, Emory University, 1365 Clifton Road, Atlanta, GA 30322; ophtheg@emory.edu.

Materials and Methods

Cells

Human uveal melanoma Mel290, Mel270, OMM2.3 (courtesy of Bruce Ksander, Schepens Eye Institute, Boston, MA), primary uveal melanoma cells from our laboratory (02-1486), human uveal melanocytes (courtesy of Dan-Ning Hu, New York Eye and Ear Infirmary, New York, NY), and mouse cutaneous melanoma B16LS9 (courtesy of Dario Rusciano, Friedrich Miescher Institute, Basel, Switzerland), B16F10, and Queens cells (courtesy of Jerry Niederkorn, UT Southwestern, Dallas, TX) were maintained in RPMI 1640 supplemented with 10% fetal bovine serum, L-glutamine, HEPES, sodium bicarbonate, vitamin, and penicillin/streptomycin.

PEDF mRNA Expression Detected by Real-Time RT-PCR

Total RNAs were extracted by reagent (TRIzol; Invitrogen, Carlsbad, CA), and resuspended in nuclease-free water. Endonuclease (RNase-free DNAse I; Qiagen, Germantown, MD) was used to remove DNA. The concentration and purity of RNA were measured with a spectrophotometer (Biomate 3; Thermo Scientific, Madison, WI). RNA was stored at −80°C. One-step real-time RT-PCR was performed using a RT-PCR kit (QuantiTect SYBR Green; Qiagen, Valencia, CA) on a thermocycler (iCycler; Bio-Rad, Hercules, CA). The primers were designed by primer software (Primer Express; Applied Biosystems, Foster City, CA). The GenBank accession number of mouse PEDF is NM_011340. Primers for the detection of mouse PEDF mRNA were 5′-TCG AAA GCA GCC CTG TGT T-3′ and 5′-AAT CAC CCG ACT TCA GCA AGA-3′. The GenBank accession number of human PEDF is NM_002615. Primers for the detection of human PEDF mRNA were 5′-TAT GAC CTG TAC CGG GTG CGA T-3′ and 5′-CCA CAC TGA GAG GAG ACA GGA GC-3′. β-Actin was selected as the internal control reference gene. Sequences of mouse β-actin primers were 5′-AAG TGT GAC GTT GAC ATC CGT AA-3′ and 5′-TGC CTG GGT ACA TGG TGG TA-3′, and of human β-actin primers they were 5′-CCT GGC ACC CAG CAC AAT G-3′ and 5′-CGC CGA TCC ACA CGG AGT AC-3′. Ten nanograms total RNA from melanoma cells was mixed with 2 μL RT-PCR master mix (QuantiTect SYBR Green; Qiagen) containing DNA Polymerase (HotStarTaq; Qiagen), Tris-HCl, KCl, $(NH_4)_2SO_4$, 5 mM $MgCl_2$, dNTP mix, SYBR Green I, and ROX, 0.3 μM of each specific primer, and 0.25 μL probe (QuantiTect RT; Qiagen) to a volume of 20 μL. The following PCR cycle parameters were used: hot-start polymerase activation for 15 minutes at 95°C and denaturation 94°C 35 seconds, annealing at 58.5°C for 30 seconds, extension at 72°C for 20 seconds; total, 40 cycles. All the samples were triplicated and run in the same 96-well plate including series of RNA dilutions for standard curves. Fluorescence product detection was performed during all the cycles. To confirm specificity, the PCR products from each pair of primers were subjected to a melt-curve analysis. Quantification data were analyzed with thermocycler system software (iCycleriQ; Bio-Rad).

Immunofluorescence

Immunofluorescence staining of frozen ocular tissue sections was performed in the mouse experiment. Intratumoral microvessels were detected with the primary antibody CD31 conjugated with FITC (BD PharMingen, San Jose, CA) and counterstained with propidium iodide. Mean microvessel density was determined by total vessel length or number of $CD31^+$ vascular capillaries per high-power field (40× magnification) using image analysis software (Image-Pro Plus 6; Media Cybernetics, Silver Spring, MD).

Transfection Efficiency

Lentiviral flap-Ub promoter-EGFP-WRE vector (courtesy of Guofo Fang, Neurodegenerative Disease Center, Emory University, Atlanta, GA) was transfected into B16LS9. When the cells reached 30% to 50% confluence, they were seeded into a six-well-plate. At 24 hours after transfection, the medium was changed with fresh complete medium. Transfection efficiency was observed daily with an inverted fluorescence microscope (Eclipse E300; Nikon, Tokyo, Japan) and was determined by counting the total number of cells without a fluorescent filter and the number of green fluorescent protein (GFP) cells with a green fluorescent filter (560 nm) in the same field under inverted fluorescence microscopy.

Lentiviral Vector Design and Production

Lentiviral expression vectors were constructed (ViraPower Lentiviral System; Invitrogen). To generate an entry clone, the mouse PEDF gene-expressive sequence was subcloned (pBLAST49-mPEDF version 13; InvivoGen, San Diego, CA) for an entry vector (pENTR/D-TOPO; Invitrogen). The sequence of the forward primer was 5′-*CACC ATG* CAG GCC CTG GTG CTA-3′, and that of the reverse PCR primer was 5′-*CTA* GCA GCT TCC CTC TGG GGT T-3′. To enable directional cloning, in the forward PCR primer, CACC was added to the 5′ end of the primer that matched the base pair with the overhanging sequence, GTGG, in the pENTR/D-TOPO vector. pLenti6.2/N-Lumio/V5-DEST allowed expression of recombinant proteins with an N-terminal peptide containing an ATG initiation codon. An ATG initiation codon after the overhanging sequence was added. The first three base pairs of the PCR product after the 5′ CACC overhang constituted a functional codon. The reverse PCR primer was not complementary to the overhanging GTGG sequence at the 5′ end and contained a stop codon (TAG). The PCR reaction was performed using a polymerase kit (HotStar HiFidelity; Qiagen) as follows: 10 ng DNA pBLAST49-mPEDF was mixed with 10 μL 5× PCR buffer, 1 μL 50 μM forward primer, 1 μL 50 μM reverse primer, and 2.5 U HotStar DNA *Taq* polymerase, and water was added to a volume of 50 μL. The following cycling parameters were used: hot-start polymerase activation for 5 minutes at 95°C, denaturation at 94°C for 30 seconds, annealing at 68°C for 1 minute, extension at 72°C for 2 minutes, total 40 cycles, and final extension was performed at 72°C for 10 minutes. The TOPO cloning reaction was performed to insert the PCR product into the entry vector pENTR/D-TOPO. Transformants were analyzed by sequencing. The resultant 1500-bp fragment was confirmed by sequencing and comparing with the sequence of the mouse PEDF gene expression region in GenBank (NM_011340.2). To create a pLenti6.2/N-Lumio/V5-DEST/mPEDF expression clone, the LR recombination reaction was performed using the attL-containing entry clone pENTR/D-TOPO/mPEDF and the attR-containing pLenti6.2/N-Lumio/V5-DEST vector, One Shot Stbl3 Competent *Escherichia coli* was transformed, and the positive clones were sequenced to confirm the sequence and position of the mouse PEDF gene with a cytomegalovirus forward primer and the PGK reverse primer. To produce lentiviral stock, 293FT cells (Invitrogen) were plated in 10-cm tissue culture plates. When they were 90% to 95% confluent, the complete culture medium was removed, and the cells were exposed to 5 mL medium (Opti-MEM I; Invitrogen) with complexes (DNA-Lipofectamine 2000; Invitrogen) containing 9 μg packaging mix (ViralPower; Invitrogen), 3 μg expression plasmid DNA (pLenti6.2/N-Lumio/V5-DEST/mPEDF), or control plasmid DNA (pLenti6.2/N-Lumio/V5-DEST/LacZ) with lipofectamine (Lipofectamine 2000; Invitrogen). Hexadimethrine bromide (Polybrene; Sigma-Aldrich, St. Louis, MO) was added at the final concentration of 10 μg/mL. After incubation for 24 hours, the infection medium was replaced with complete culture medium. Lentivirus-containing supernatants were harvested at 72 hours after transfection. The supernatants was centrifuged to remove pellet debris and stored at −80°C.

In Vitro Lentiviral Vector Transduction

After this, 10^6 B16LS9 cells were plated in each well of a 6-well-plate. When the cells reached 30% to 50% confluence, media were changed to complete growth medium without antibiotic with the lentiviral stock, and 10 μg/mL hexadimethrine bromide (Polybrene; Sigma-Aldrich) was added to improve lentiviral vector transduction. Lentiviral vector expressing lacZ served as a positive control. After incubation

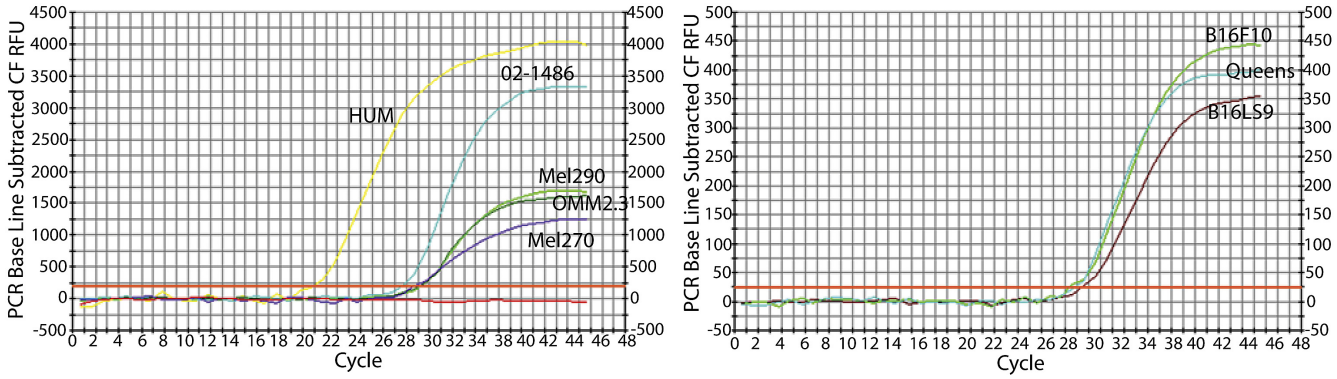

FIGURE 1. PEDF mRNA expression in human and mouse melanoma cells. PEDF mRNA expression was detected by real-time RT-PCR. Human uveal melanoma cells (*left*) have lower expression of PEDF than human uveal melanocytes (HUM, *yellow curve*). After normalization to the internal control reference gene β-actin and human uveal melanocytes, the values of ΔΔCt in Mel290, Mel270, OMM2.3, and 02–1486 are 4.23, 4.19, 3.15, and 3.74, respectively. After normalization to the internal control reference gene β-actin, the values of Δ in B16LS9, B16F10, and Queens are 5.02, 3.73, and 3.88, respectively. Mouse melanoma cells also express low levels of PEDF (*right*).

overnight at 37°C in 5% CO_2, the media-containing virus was removed and replaced with 2 mL complete culture media. After incubation overnight at 37°C in 5% CO_2, media were changed to complete growth media without antibiotic and with 4 μg/mL antibiotic (Blasticidin; InvivoGen). Transduced cell clones were selected with 4 μg/mL antibiotic (Blasticidin; InvivoGen) for 2 weeks, and cells were expanded in complete culture medium with antibiotic (Blasticidin; InvivoGen). PEDF expression was verified by quantitative real time RT-PCR, Western blot analysis, and Lumio-tagged PEDF protein in live B16LS9 cells.

Western Blot Analysis

Cell pellets were dissolved with cell extraction buffer (Biosource, Camarillo, CA). Samples were incubated for 30 minutes at 4°C and then centrifuged at 13,000 rpm for 10 minutes at 4°C. The protein concentration of the supernatant was determined by the DC protein assay (Bio-Rad Laboratories). All samples were then diluted in the 4× sample buffer (Invitrogen) and boiled. Ten micrograms of each sample was loaded on a 4% to 12% Bis-Tris gel (Novex NuPAGE; Invitrogen) and transferred onto polyvinylidene difluoride membranes (Invitrogen). The membranes were blocked with blocking buffer (Pierce, Rockford, IL) for 1 to 2 hours at room temperature. Membranes were reacted with anti-PEDF antibody (Santa Cruz Biotechnology, Santa Cruz, CA) or anti-V5 (Invitrogen) or β-actin (Sigma) antibodies overnight at 4°C, after 1 hour of horseradish peroxidase-conjugated secondary antibody incubation. Immunoreactive bands were detected after washes in Tris-buffered saline with Tween 20.

Transendothelial Migration and Melanoma Tube Formation Assay

Transendothelial migration assays were performed with an assay kit (CytoSelect Tumor Transendothelial Migration Assay Kit; Cell Biolabs, Inc. San Diego, CA). Murine vascular endothelial cells were plated onto 8-μm pore size inserts in 24-well plates and allowed to form a confluent monolayer on the membrane for 72 hours. After B16LS9-PEDF, B16LS9-LacZ, and B16LS9 cells were marked (CytoTracker; Molecular Probes, Eugene, OR), they were plated onto the endothelial cell monolayer in the upper inserts via bottom inserts containing RPMI with or without 10% FBS. The tumor cells were allowed to transmigrate through the endothelium and the membrane overnight. Nonmigratory cells were removed and migratory cells were lysed. Fluorescence was determined with a fluorescence plate reader at 480 nm/520 nm.

B16LS9-mPEDF, B16LS9-LacZ, and B16LS9 cells were plated (ECMatrix Gel; (Millipore, Billerica, MA), incubated at 5% CO_2 at 37°C for 22 hours, and inspected for tube formation under an inverted light microscope. The value of tube pattern was classified according to the manufacturer's manual. The pattern/value association criteria were: 0, individual cells, well separated; 1, cells beginning to migrate and align themselves; 2, capillary tubes visible without sprouting; 3, sprouting of new capillary tubes visible; 4, closed polygons beginning to form; 5, complex meshlike structures developing. Three random fields per well were examined at 100× magnification, and the values were averaged.

Mouse Ocular Melanoma Model

All animal procedures performed in this study complied with the ARVO Statement for the Use of Animals in Ophthalmic and Vision Research. Stably PEDF-overexpressing B16LS9 (B16LS9-mPEDF; 5×10^5) or vehicle control B16LS9 (B16LS9-LacZ) or control B16LS9 cells were inoculated into the posterior compartment of the right eye in C57BL/6 mice. The eye was enucleated at 7 days after inoculation, fixed in 10% formalin, and routinely processed for light microscopic examination. Serially adjacent 5-μm-thick sections were stained with hematoxylin and eosin and evaluated for the presence and location of melanoma. Ten sections with the largest tumor area in each eye were photographed (DP10; Olympus Tokyo, Japan). The sizes of the intraocular tumors were determined with ImageJ software (developed by Wayne Rasband, National Institutes of Health, Bethesda, MD; available at http://rsb.info.nih.gov/ij/index.html). Hepatic tissue was collected 4 weeks after inoculation, submitted in 10% formalin, and routinely processed for light microscopic examination, and the number of hepatic micrometastases was enumerated as previously described.[32,33] B16LS9 orthografts were used rather than human uveal melanoma xenografts because B16LS9 cells display biological behavior similar to that of human uveal melanoma cells that metastasize to the liver without the immune suppression needed in a xenograft model.[33] We have previously shown that the histogically identified hepatic micrometastases correspond to GFP-labeled micrometastases originating from tumor in the eye.[34] Fifteen mice in each group were inoculated with the three different B16LS9 cells (B16LS9-mPEDF, B16LS9-LacZ, B16LS9). This experiment was repeated twice.

RESULTS

Expression of PEDF by Human Uveal Melanoma and Mouse Melanoma Cells

A low level of PEDF mRNA was detected in Mel290, Mel270, OMM 2.3 and 02–1486 human uveal melanoma cells and in B16LS9, B16F10, and Queens mouse melanoma cells by real-time RT-PCR (Fig. 1). PEDF mRNA values were normalized to β-actin according to Pfaffl's mathematical model for relative quantification in real-time PCR.[35] The levels of PEDF mRNA in human uveal melanoma cells were <0.10, but the level of

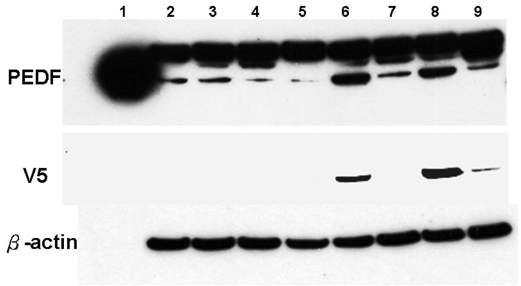

FIGURE 2. Transfected B16LS9 melanoma cells overexpress PEDF protein. Lentiviral-mediated PEDF gene-transfected clones were characterized for PEDF production by Western blot analysis. *Lane 1* was loaded with recombinant PEDF protein (10 ng) used as the positive control, *lane 2* was loaded the lysate from B16LS9 control cells, *lanes 3-8* were loaded with the lysates from different B16LS9-mPEDF cell clones, and *lane 9* was loaded the lysate from the B16LS9-LacZ-transfected control cells. Overexpression of PEDF was demonstrated in *lanes 6* and *8*. V5 expression loaded with the lysate from a vehicle control, B16LS9-LacZ, was determined in *lanes 6, 8,* and *9*. β-Actin served as a control.

PEDF mRNA in human uveal melanocytes was 0.36. The levels of PEDF mRNA in B16LS9, B16F10. and Queens were 0.049, 0.058, and 0.052, respectively.

Efficient Transfection of B16LS9 by Lentiviral Vector EGFP

We first asked whether the lentiviral vectors could efficiently mediate transgene expression in the mouse melanoma B16LS9 cell line. Lentiviral flap-Ub promoter-EGFP-WRE vector was transfected into the mouse melanoma B16LS9 cell line. At 24 hours after transfection, EGFP expression was observed by inverted fluorescence microscopy. At 72 hours after transfection, 50% to 70% of B16LS9 expressed EGFP. At 45 days, 6 passages, 50% to 70% of B16LS9 stably expressed EGFP.

Establishment of B16LS9 Cells with Stable mPEDF Expression

The expression sequence of the mouse PEDF gene was amplified by PCR from pBLAST49-mPEDF v13. The length of the amplified expression fragment was 1286 bp. The amplified expression fragment was inserted into pLenti6.2/N-Lumio/V5-DEST, to produce the mouse PEDF expression vector that we called pLenti6.2/N-Lumio/V5-DEST/mPEDF. Sequencing results for the pLenti6.2/N-Lumio/V5-DEST/mPEDF vector showed that the sequence of the 1286bp PCR product matched the mouse PEDF gene expression sequence, (GenBank accession number, NM_011340.2). After the PLENTI6.2/N-LUMIO/V5-DEST/MPEDF vector was transfected into B16LS9 cells, transfected B16LS9 cells were resistant to (Blasticidin; InvivoGen) and able to live in complete culture medium with (Blasticidin; InvivoGen), whereas nontransfected cells were killed. Transfected cells expanded and formed cell clones on the 14th day after transfection. Isolated cell clones were separated to different cell culture dishes and continued expanding.

Overexpression of PEDF by Transfected B16LS9 Melanoma Cells

Real-time RT-PCR confirmed that the level of PEDF mRNA was increased in B16LS9 cells after transfection with the pLenti6.2/N-Lumio/V5-DEST/mPEDF vector (B16LS9-mPEDF), compared with B16LS9 after transfection with the pLenti6.2/N-Lumio/V5-DEST/lacZ vector (B16LS9-LacZ and B16LS9). Stably transduced clones were expanded. The lysates from mouse melanoma B16LS9-mPEDF, B16LS9-LacZ, and B16LS9 cell lines were subjected to Western blot analysis, which showed that compared with B16LS9-LacZ and B16LS9, the PEDF protein was overexpressed in B16LS9-mPEDF cells (Fig. 2, lanes 6–8). The clones with V5 tag expression and PEDF overexpression, in which the levels of PEDF mRNA were upregulated >2.5-fold, were used for further in vitro and in vivo experiments.

Decreased Transendothelial Migration in PEDF-Transduced B16LS9 Melanoma Cells

There was a significant difference in the value of relative fluorescence units (RFUs) from B16LS9 transduced by lentivirus-mediated PEDF compared with vehicle control B16LS9 transduced by lentivirus-mediated LacZ ($P < 0.01$) and control B16LS9 cells and no significant difference in the RFUs between the vehicle LacZ and control cells ($P > 0.05$, Fig. 3).

Decreased Tube Formation in Transduced B16LS9 Melanoma Cells

The total length of all the tubes was measured per well in triplicate for each cell by ImageJ. The total length of all the tubes produced by B16LS9-mPEDF, B16LS9-LacZ, and B16LS9 were 76 ± 14 pixels, 890 ± 91 pixels, and 830 ± 61 pixels, respectively. The ability of tube formation in B16LS9-mPEDF was significantly reduced compared with B16LS9-LacZ and B16LS9 cells ($P < 0.01$) The values of the patterns were separately recognized as 1, 4, and 4 in B16LS9-mPEDF, B16LS9-LacZ, and B16LS9 cells, respectively (Fig. 4). B16LS9-mPEDF cells did not form tubes.

PEDF Inhibition of Growth of Ocular Melanoma and Number of Hepatic Micrometastasis in a Mouse Uveal Melanoma Model

The size of mouse ocular tumor was measured by ImageJ. Average areas of ocular tumor were 133,404 ± 19,430 pixel^2, 303,738 ± 40,536 pixel^2, and 497,782±129,479 pixel^2 in the eye inoculated with B16LS9-mPEDF, B16LS9-LacZ, and B16LS9 cells, respectively (Figs. 5A–C). The size of the ocular tumor in mice inoculated with B16LS9-mPEDF cells was significantly lower than in mice inoculated with B16LS9-LacZ or B16LS9 cells ($P < 0.01$). The number of capillaries of the ocular tumors inoculated with B16LS9-mPEDF cells (81.67 ± 22.50) was lower than those inoculated with B16LS9-LacZ cells (215.67 ± 54.79, $P = 0.0086$; Figs. 5E, 5F). The sum of capillary length in the ocular tumors inoculated with B16LS9-mPEDF cells (492.71 ± 93.11 μm) was significantly lower than of mice

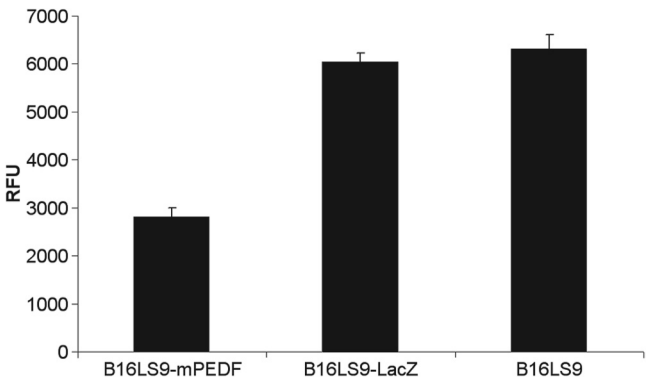

FIGURE 3. Decreased transendothelial migration of transfected B16LS9 melanoma cells. The average calibrated values of RFU in B16LS9-mPEDF, B16LS9-LacZ, and B16LS9 were 2805 ± 197, 6030 ± 282, and 6305 ± 305, respectively. The average RFU value in B16LS9-mPEDF cells was significantly lower than in B16LS9 cells ($P < 0.01$). The values of RFU were read by a fluorescence plate reader at 480 nm/520 nm and were corrected with background control wells.

FIGURE 4. In vitro angiogenesis assay. Closed polygons formed and were graded as a value of 4 in B16LS9 and B16LS9-LacZ cells. B16LS9-mPEDF cells migrated, aligned themselves, and were graded as value 1. B16LS9-mPEDF lost the ability to form tubes.

inoculated with B16LS9-LacZ cells (1205.16 ± 26.34, $P = 0.00024$). After establishing the mouse ocular melanoma model with B16LS9-mPEDF, B16LS9-LacZ, and B16LS9 cells, histologic examination showed that the number of hepatic micrometastasis in group 1 inoculated with B16LS9-mPEDF cells (42 ± 21) was significantly lower than the number of hepatic micrometastasis in group 2 inoculated with B16LS9-LacZ cells (116 ± 75) and in group 3 inoculated with B16LS9 (81 ± 36). Statistical analysis demonstrated that there was a significant difference in the number of hepatic micrometastasis in group 1 compared with group 2 ($P = 0.006$) and group 3 ($P = 0.001$) and no difference in the number of hepatic micrometastasis in group 2 compared with group 3 ($P = 0.15$; Fig. 5D).

DISCUSSION

PEDF was purified in 1987 in conditioned medium from fetal human retinal pigment epithelium cell culture.[36] It was originally described as a potent antiangiogenic protein. Angiogenesis, a process in which new vascular networks are formed from preexisting capillaries, is required for tumor growth, invasion, and metastasis. Recent studies have shown that PEDF is able to inhibit angiogenesis in various tumors. Adenocarcinoma of the prostate and pancreas and osteosarcoma secrete PEDF. We found that human uveal melanoma cells and mouse melanoma cells express endogenous PEDF in vitro and that some uveal melanoma cells express PEDF in situ.

Exogenous PEDF has direct and indirect antitumor mechanisms of action.[31] The direct mechanisms of action include promotion of tumor differentiation[36] and an antitumor cell migration effect.[37] The indirect antitumor effect is inhibition of tumor angiogenesis. A reduction in the in vitro migratory potential of cutaneous melanoma cells overexpressing PEDF has been reported. Similar results have been reported in glioma, in which PEDF overexpression downregulates matrix metalloproteinase-9, which may account for reduced invasiveness.[24,25] In our study, we verified that endogenous overexpression of PEDF inhibits transendothelial migration in vitro. We also showed that endogenous overexpression of PEDF in melanoma cells reduces the size of the intraocular tumor and the number of hepatic micrometastases in a mouse ocular melanoma model. Our results suggest that increasing the level of endogenous PEDF may provide an effective approach for the treatment of primary ocular melanoma and the prevention of metastasis.

Angiogenesis is necessary for tumor growth and is a critical component of tumor metastasis. Highly vascularized tumors have the potential to produce metastases at a higher rate than less vascularized tumors. The generation of hematogenous spread of a tumor requires tumor cell proliferation, angiogenesis, and invasion of tumor vascular channels. Tumor cell proliferation alone, coupled with steady state apoptosis, in the absence of angiogenesis, gives rise to dormant, microscopic tumors measuring approximately 1 mm^3 or less. These dormant micrometastases are harmless to the host.[38–44] Transfection of an oncogene into tumor cells may increase angiogenic activity by increasing tumor expression of vascular endothelial growth factor (VEGF) and by decreasing expression of antiangiogenic proteins,[44,45] such as PEDF, which has been identified as the most potent endogenous inhibitor of angiogenesis in the mammalian eye.

There is a balance between angiogenesis activation and inhibition of tumor progression via antiangiogenesis. The balance is shifted toward angiogenesis if the effects of angiogenesis activators exceed the effects of angiogenesis inhibitors.[46–48] Angiogenesis is controlled by a coordinated production of endogenous angiogenesis activators and inhibitors.[48] The balance between PEDF and VEGF plays a role in the development of angiogenesis in tumors. Melanoma cells share important cell surface molecules with endothelial cells and may exhibit a vascular phenotype[49] imitating vessel formation. Our melanoma tube formation assay showed decreased tube formation in vitro and showed that endogenous overexpression of PEDF reduced the number and total length of microvessels in the ocular tumor in mouse model. These results imply that PEDF may play a role in the downregulation of tube formation and fluid circulation within uveal melanoma.

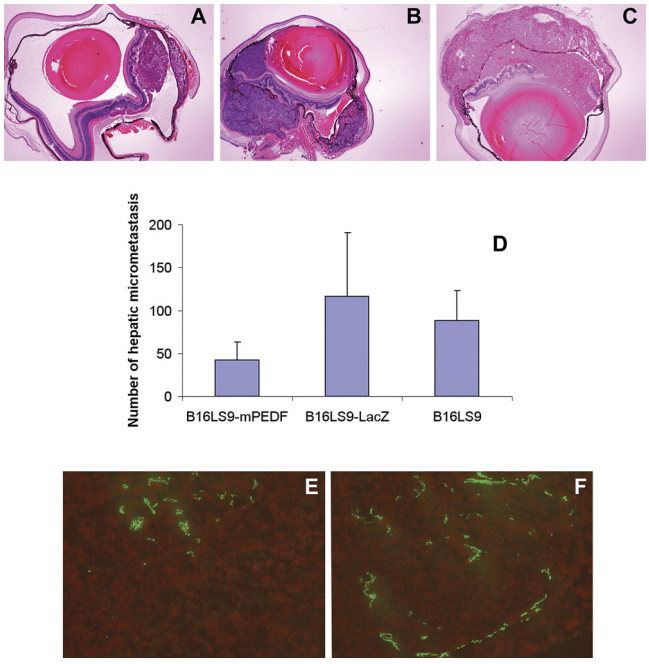

FIGURE 5. Endogenous overexpression of PEDF inhibited B16LS9 ocular tumor and hepatic micrometastasis in vivo. Intraocular tumors in mice inoculated with B16LS9-mPEDF (**A**) were smaller than those inoculated with B16LS9-LacZ (**B**) or B16LS9 (**C**) (hematoxylin and eosin stain, 40×). There were fewer hepatic micrometastases in the B16LS9-mPEDF- than the B16LS9-LacZ- or B16LS9-inoculated mice (**D**). There were fewer $CD31^+$ vascular channels in the B16LS9-mPEDF (**E**) than in the B16LS9-LacZ (**F**) mice. CD31, red fluorescence; propidium iodide counterstain, 200×.

In our study, increasing the level of PEDF resulted in decreased angiogenesis and decreased melanoma size. We constructed a lentiviral vector capable of efficient transduction and expression of PEDF in mouse melanoma cells and established a melanoma cell line with stable overexpression of PEDF. Our results show that the melanoma cells overexpressing PEDF exhibit decreased transendothelial migration and lose their ability to form tubes in vitro and that microvessel density is decreased in the ocular tumor created by the inoculation of PEDF-overexpressing melanoma cells. These findings imply that PEDF-directed therapies offer a promising avenue for the prevention and treatment of uveal melanoma micrometastasis. The molecular mechanisms of PEDF antimelanoma growth and metastasis warrant further investigation.

References

1. Singh AD, Bergman L, Seregard S. Uveal melanoma: epidemiologic aspects. *Ophthalmol Clin North Am.* 2005;18:75–84.
2. Singh AD, Topham A. Incidence of uveal melanoma in the United States: 1973–1997. *Ophthalmology.* 2003;110:956–961.
3. Tombran-Tink J, Johnson LV. Neuronal differentiation of retinoblastoma cells induced by medium conditioned by human RPE cells. *Invest Ophthalmol Vis Sci.* 1980;30:1700–1707.
4. Steele FR, Chader GJ, Johnson LV, Tombran-Tink J. Pigment epithelium-derived factor: neurotrophic activity and identification as a member of the serine protease inhibitor gene family. *Proc Natl Acad Sci U S A.* 1992;90:1526–1530.
5. Tombran-Tink J, Pawar H, Swaroop A, Rodriguez I, Chader GJ. Localization of the gene for pigment epithelium-derived factor (PEDF) to chromosome 17p13.1 and expression in cultured human retinoblastoma cells. *Genomics.* 1994;19:266–272.
6. Dawson DW, Volpert OV, Gillis P, et al. Pigment epithelium-derived factor: a potent inhibitor of angiogenesis. *Science.* 1999; 285:245–248.
7. Sawant S, Aparicio S, Tink AR, Lara N, Barnstable CJ, Tombran-Tink J. Regulation of factors controlling angiogenesis in liver development: a role for PEDF in the formation and maintenance of normal vasculature. *Biochem Biophys Res Commun.* 2004;325: 408–413.
8. Quan GM, Ojaimi J, Li Y, Kartsogiannis V, Zhou H, Choong PF. Localization of pigment epithelium-derived factor in growing mouse bone. *Calcif Tissue Int.* 2005;76:146–153.
9. Bilak MM, Corse AM, Bilak SR, Lehar M, Tombran-Tink J, Kuncl RW. Pigment epithelium-derived factor (PEDF) protects motor neurons from chronic glutamate-mediated neurodegeneration. *J Neuropathol Exp Neurol.* 1999;58:719–728.
10. Kuncl RW, Bilak MM, Bilak SR, Corse AM, Royal W, Becerra SP. Pigment epithelium-derived factor is elevated in CSF of patients with amyotrophic lateral sclerosis. *J Neurochem.* 2002;81:178–184.
11. Tombran-Tink J, Mazuruk K, Rodriguez IR, et al. Organization, evolutionary conservation, expression and unusual Alu density of the human gene for pigment epithelium-derived factor, a unique neurotrophic serpin. *Mol Vis.* 1996;2:11.
12. Yang H, Xu Z, Iuvone PM, Grossniklaus HE. Angiostatin decreases cell migration and vascular endothelium growth factor (VEGF) and pigment epithelium derived factor (PEDF) RNA ratio in vitro and in a murine ocular melanoma model. *Mol Vis.* 2006;22:511–517.
13. Ortego J, Escribano J, Becerra SP, Coca-Prados M. Gene expression of the neurotrophic pigment epithelium-derived factor in the human ciliary epithelium: synthesis and secretion into the aqueous humor. *Invest Ophthalmol Vis Sci.* 1996;37:2759–2767.
14. Behling KC, Surace EM, Bennett J. Pigment epithelium-derived factor expression in the developing mouse eye. *Mol Vis.* 2002;18: 449–454.
15. Mori K, Duh E, Gehlbach P, et al. Pigment epithelium-derived factor inhibits retinal and choroidal neovascularization. *J Cell Physiol.* 2001;188:253–263.
16. Raisler BJ, Berns KI, Grant MB, et al. Adeno-associated virus type-2 expression of pigmented epithelium-derived factor or Kringles 1–3 of angiostatin reduce retinal neovascularization. *Proc Natl Acad Sci U S A.* 2002;99:8909–8914.
17. Tsao YP, Ho TC, Chen SL, Cheng HC. Pigment epithelium-derived factor inhibits oxidative stress-induced cell death by activation of extracellular signal-regulated kinases in cultured retinal pigment epithelial cells. *Life Sci.* 2006;79:545–550.
18. Yamagishi S, Matsui T, Nakamura K, et al. Pigment-epithelium-derived factor suppresses expression of receptor for advanced glycation end products in the eye of diabetic rats. *Ophthalmic Res.* 2007;39:92–97.
19. Cai J, Parr C, Watkins G, Jiang WG, Boulton M. Decreased pigment epithelium-derived factor expression in human breast cancer progression. *Clin Cancer Res.* 2006;12:3510–3517.
20. Doll JA, Stellmach VM, Bouck NP, et al. Pigment epithelium-derived factor regulates the vasculature and mass of the prostate and pancreas. *Nat Med.* 2003;9:774–780.
21. Uehara H, Miyamoto M, Kato K, et al. Expression of pigment epithelium-derived factor decreases liver metastasis and correlates with favorable prognosis for patients with ductal pancreatic adenocarcinoma. *Cancer Res.* 2004;64:3533–3537.
22. Halin S, Wikstrom P, Rudolfsson SH, et al. Decreased pigment epithelium-derived factor is associated with metastatic phenotype in human and rat prostate tumors. *Cancer Res.* 2004;64:5664–5671.
23. Crawford SE, Stellmach V, Ranalli M, et al. Pigment epithelium-derived factor (PEDF) in neuroblastoma: a multifunctional mediator of Schwann cell antitumor activity. *J Cell Sci.* 2001;114:4421–4428.
24. Guan M, Yam HF, Su B, et al. Loss of pigment epithelium derived factor expression in glioma progression. *J Clin Pathol.* 2003;56: 277–282.
25. Guan M, Pang CP, Yam HF, et al. Inhibition of glioma invasion by overexpression of pigment epithelium-derived factor. *Cancer Gene Ther.* 2004;11:325–332.
26. Garcia M, Fernandez-Garcia NI, Rivas V, et al. Inhibition of xenografted human melanoma growth and prevention of metastasis development by dual antiangiogenic/antitumor activities of pigment epithelium-derived factor. *Cancer Res.* 2004;64:5632–5642.
27. Browne M, Stellmach V, Cornwell M, et al. Gene transfer of pigment epithelium-derived factor suppresses tumor growth and angiogenesis in a hepatoblastoma xenograft model. *Pediatr Res.* 2006;60:282–287.
28. Takenaka K, Yamagishi S, Jinnouchi Y, et al. Pigment epithelium-derived factor (PEDF)-induced apoptosis and inhibition of vascular endothelial growth factor (VEGF) expression in MG63 human osteosarcoma cells. *Life Sci.* 2005;77:3231–3241.
29. Ek ET, Dass CR, Contreras KG, Choong PF. Pigment epithelium-derived factor overexpression inhibits orthotopic osteosarcoma growth, angiogenesis and metastasis. *Cancer Gene Ther.* 2007;14: 616–626.
30. Abe R, Shimizu T, Yamagishi S, et al. Overexpression of pigment epithelium-derived factor decreases angiogenesis and inhibits the growth of human malignant melanoma cells in vivo. *Am J Pathol.* 2004;164:1225–1232.
31. Garcia M, Fernandez-Garcia NI, Rivas V, et al. Inhibition of xenografted human melanoma growth and prevention of metastasis development by dual antiangiogenic/antitumor activities of pigment epithelium-derived factor. *Cancer Res.* 2004;64:5632–5642.
32. Dithmar S, Rusciano D, Grossniklaus HE. A new technique for implantation of tissue culture melanoma cells in a murine model of metastatic ocular melanoma. *Melanoma Res.* 2000;10:2–8.
33. Dithmar S, Grossniklaus HE, Albert DM. Animal models of uveal melanoma. *Melanoma Res.* 2000;10:195–211.
34. Yang H, Fang G, Huang X, et al. In-vivo xenograft murine human uveal melanoma model develops hepatic micrometastases. *Melanoma Res.* 2008;18:95–103.
35. Pfaffl MW. A new mathematical model for relative quantification in real-time RT-PCR. *Nucleic Acids Res.* 2001;29:2002–2007.
36. Tombran-Tink J, Johnson LV. Neuronal differentiation of retinoblastoma cells induced by medium conditioned by human RPE cells. *Invest Ophthalmol Vis Sci.* 1989;30:1700–1707.
37. Fernandez-Garcia NI, Volpert OV, Jimenez B. Pigment epithelium-derived factor as a multifunctional antitumor factor. *J Mol Med.* 2007;85:15–22.

38. Gimbrone MA Jr, Leapman SB, Cotran RS, et al. Tumor dormancy in vivo by prevention of neovascularization. *J Exp Med.* 1972;136: 261–276.
39. Brem S, Brem H, Folkman J, et al. Prolonged tumor dormancy by prevention of neovascularization in the vitreous. *Cancer Res.* 1976;36:2807–2812.
40. Holmgren L, O'Reilly MS, Folkman J. Dormancy of micrometastases: balanced proliferation and apoptosis in the presence of angiogenesis suppression. *Nat Med.* 1995;1:149–153.
41. Hanahan D, Folkman J. Patterns and emerging mechanisms of the angiogenic switch during tumorigenesis. *Cell.* 1996;86:353–364.
42. Arbiser JL, Moses MA, Fernandez CA, et al. Oncogenic H-ras stimulates tumor angiogenesis by two distinct pathways. *Proc Natl Acad Sci USA.* 1997;94:861–866.
43. Folkman J. Incipient angiogenesis. *J Natl Cancer Inst.* 2000;92: 94–95.
44. Folkman J. *Angiogensis Annu Rev Med.* 2006;57:1–18.
45. Watnick RS, Cheng Y-N, Rangarajan A, et al. Ras modulates Myc activity to repress thrombospondin-1 expression and increase tumor angiogenesis. *Cancer Cell.* 2003;3:219–231.
46. Connell RD. Patent focus on cancer chemotherapeutics, V: angiogenesis agents: September 2001–August 2002. *Exp Opin Ther Patents.* 2002;12:1763–1782.
47. Mousa SA. Mechanisms of angiogenesis in vascular disorders: potential therapeutic targets. *Drugs Fut.* 1998;23:51.
48. Paper DH. Natural products as angiogenesis inhibitors. *Planta Med.* 1998;64:686–695.
49. Velazquez OC, Herlyn M. The vascular phenotype of melanoma metastasis. *Clin Exp Metast.* 2003;20:229–235.